The 12th IEEE International Conference on Intelligent Data Acquisition and Advanced Computing Systems: Technology and Applications
7-9 September, 2023, Dortmund, Germany

Suppressing Laser Triangulation Sensors Optical Aberrations by Replacing the Lens with a Slit

Benjamin Lapointe-Pinel[1] , Steven Pigeon[2]
Université du Québec à Rimouski, 300 allée des Ursulines, Rimouski QC G5L 3A1, Canada
[1] Benjamin.Lapointe-Pinel@uqar.ca
[2] Steven_Pigeon@uqar.ca

Abstract — This paper presents a new capture method for laser triangulation sensors consisting in replacing the lens with a slit—effectively making it a pinhole camera—and exploiting diffraction effects. This new method circumvents optical aberrations such as spherical, defocusing, coma, field curvature, and lens distortion, as well as lens flare to a point where it can be virtually ignored. Moreover, using a slit reduces the number of optical parts and simplifies the modeling of the laser spot to find its center. To test our proposed method, we generated data sets taking pictures with both a lens and a slit on different materials placed on a worm gear with its position controlled by a high-precision step motor. With this data, we extracted the center of the laser spot with different image processing algorithms. It was then possible to assess the goodness of fit of the triangulation curve using the sets of captured points by both methods. We show that not only we circumvent the adverse effects of optical aberrations and lens flares, we obtain a more accurate estimation of the actual known distance of the target.

Keywords — diffraction; displacement sensor; distance measurement; laser; laser triangulation; lens; non-contact measurement; optical aberration; optics; pinhole camera; pinhole optics; range sensor; sensor; triangulation

I. Introduction

In many settings, we are interested in measuring the distance without contact between a point on an object and a sensor. When large distances are involved, time-of-flight camera are typically used, where the time between the emission of a laser and the detection of its reflection is measured, usually with an accuracy in the order of millimeters [1]–[4]. Laser triangulation sensors are commonly used when centimeter-scale distances are involved to obtain greater accuracy, well within micrometers [5]–[11]. In such sensors, a laser beam and a photosensitive sensor are placed at an angle to each other. The laser beam is reflected by a target to the photosensitive sensor, and because the horizontal axis of the sensor is parallel to the plane defined by the optical axis and the laser beam, the projection of the laser spot on the sensor only moves horizontally. Given the geometry of the system shown in Fig. 1, it is therefore possible, using triangulation, to find the distance c from the position of the laser spot on the sensor x using the relation

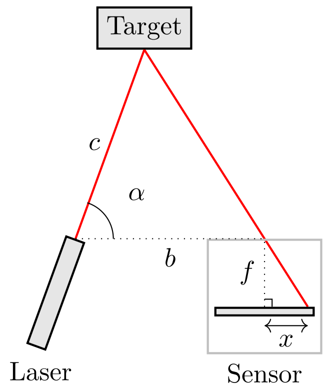

Figure 1. Laser triangulation principle.

$$c = \frac{b \sin\left(\arctan\left(f/x\right)\right)}{\sin\left(\alpha + \arctan\left(f/x\right)\right)}. \tag{1}$$

Laser triangulation commonly operate with the analysis of images taken from a sensor with a lens, which brings some challenges in the design, calibration and image analysis. Several researchers have proposed different methods to address these issues. A common approach is to angle the lens from the sensor in a way as to exploit the Scheimpflug principle to expand the depth of field along the laser beam [8], [12]. Some authors duplicated the number of cameras or sensors to make multiple readings at the same time and perform a more detailed analysis [13]–[15]. Bickel et al. and Häusler et al. replaced the laser lens with an axicon—a conical Fresnel-like lens—for a better laser depth of field [16], [17]. Žbontar et al. used a dynamic symmetrical laser ring pattern using a fast steering mirror for more precise distance measurements and to reduce speckle noise [18]. Kienle et al. split the beam in two as a way to have a reference beam to compensate for optomechanical errors [19]. Diffraction grating is used by Ye et al. as a mean to split the laser spot reflection on the sensor to allow multiple readings [20].

All current triangulation sensors use camera lens, which display a number of monochromatic optical aberrations, such as spherical, defocusing, coma, field curvature, and lens distortion, while also being susceptible to lens flare. Even though it is possible to compensate for some of these (often driving up the manufacturing cost), it may exacerbate other aberrations. One recent example, Rafael G. González-Acuña et al. found a general formula for aspherical lens free of spherical aberration [21], although such lens would still be affected by other aberrations and lens flare. All these factors complicate the manufacture, calibration, and software and influence the accuracy of the sensor. In addition, lenses require many delicate parts, which can increase costs and maintenance.

In this paper, we will show that using a pinhole camera circumvents most monochromatic optical aberrations and nearly eliminates lens flare, while simplifying manufacturing, reducing costs, and removing the need for software correction of aberrations, and that the use of a slit instead of a circular aperture reduces the influence of laser speckle.

II. Hypothesis

In papers on cameras and pinhole photography, Young shows that using a pinhole camera offers a theoretically infinite depth of field, or at least in practice, greater than a lens [22], [23]. He also shows that pinhole optics does not create any spherical optical aberration, defocusing, coma, field curvature, or distortion. It is also worth noting that a pinhole can offer a viewing angle of up to 180°, which is comparable to fisheye lenses, but without their particularly pronounced optical aberrations [24], [25]. This wider viewing angle could potentially be used to increase the range of a laser triangulation sensor. On the other hand, Young notes that the pinhole is still sensitive to astigmatism, especially when the subject is far from the center of the field of view, in which case the circular opening behaves as an ellipse. Within a restricted triangulation setting, the laser spot is constrained to move horizontally with respect to the sensor, so the astigmatism is symmetrical on the horizontal axis. Young shows, however, that the pinhole is still sensitive to chromatic aberrations. Fortunately, for an apparatus using a monochromatic camera, a bandpass filter, and a monochromatic laser, these aberrations can be neglected. In any case, a pinhole camera minimizes the possibilities of optical aberrations in the system, and simplifies the optical correction algorithms. Furthermore, since the number of optical parts is reduced, and since the pinhole acts as a spatial filter, the lens flare should dramatically decrease.

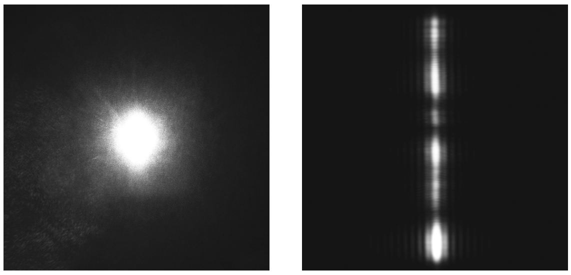

Figure 2. Left: the laser spot on sensor, right: slit diffraction pattern (contrast exaggerated for display purposes).

If we filter all light except for the laser wavelength, we will observe an Airy diffraction pattern on the sensor [26]. This would facilitate finding the center of the laser spot, since the diffraction pattern is symmetrical and does not depend on the uniformity of the spot. For a constant intensity, wavelength, and aperture, only the angle of the spot with respect to the aperture determines the position of the pattern on the sensor. Unfortunately, diffraction is particularly sensitive to speckle, a phenomenon in which laser light, after being reflected from a microscopically imperfect surface, becomes out of phase and interferes with itself, introducing noise. Ultimately, sensors using lasers are fundamentally limited by speckle [27]–[29].

To alleviate this problem, we will use a vertical slit rather than a circular aperture, retaining advantages previously cited, without additional complexity. We move from a radially symmetrical pattern to a pattern that is symmetrical only on the horizontal and vertical axes. This new diffraction pattern is in the same orientation as the slit, as shown in Fig. 2, and allows for a line-by-line analysis. This could potentially reduce the effect of speckle by averaging errors in each of the image's lines. Although the diffraction pattern will spread when the spot moves away from the center of the field of view, it will remain symmetrical, and thus will not cause any significant problems for analysis.

Therefore, our hypothesis is the following: replacing the lens with a slit improves the accuracy and range of laser triangulation sensors by bypassing most of the optical aberrations of lenses, by decreasing internal reflection, and by exploiting diffraction patterns for image analysis. As a bonus, it would reduce the manufacturing and maintenance costs, and it may reduce the need for fine calibration for these sensors.

III. Methodology

In order to generate experimental data, we built a motorized linear displacement table controlled by a desktop computer. It consists of a carriage that

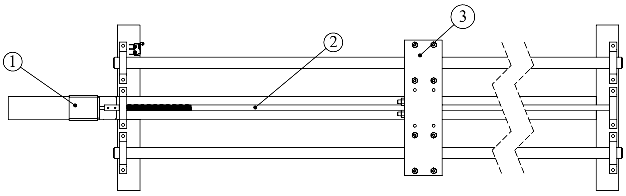

Figure 3. Top view of the experimentation table. ① is the step motor, ② is the worm gear, and ③ is the target carriage.

can support different targets, placed on a worm screw controlled by a 6400 microsteps motor. This assembly moves the target by intervals as small as 25 um without loss of precision. Indeed, after moving the carriage 25 µm 60000 times over 150 cm (the length of the worm screw), the error is under 1 mm. Thus, the precision of the displacement for one step is 25 µm ± 0.017 µm.

The laser and the camera module are placed above the motor 30 cm apart. We use a 5 mW 650 nm red laser, a common choice for this type of application. A 650 ± 8 nm bandpass filter is placed in front of the camera lens. The CMOS monochromatic camera resolution is 1920×1080 pixels, with a region of interest of 1920×600 pixels. The camera uses a 4.8×3.6 mm global shutter image sensor [30], [31]. We chose a Computar C-Mount 50 mm lens with an aperture of $f/1.8$. The 0.2×3 mm slit is also placed 50 mm from the camera sensor. The slit dimensions seem to be a good compromise between minimizing speckle noise while maximizing the diffraction pattern brightness on the sensor. We did not use the Scheimpflug technique when capturing images with the lens in order to demonstrate that the slit has a greater depth of field. Fig. 3 shows the experimentation table.

Images were captured using the same desktop computer that controls the motor. The captures were done at regular intervals of 25 µm, from a distance of 60 cm to the sensor over a range of 42 cm. The reading intervals correspond to the useful field of view of the sensor, in other words, when the laser spot happens to be fully captured. The slit field of view is wider than the lens', but both begin at 60 cm from the sensor. The pictures were labeled with their relative displacement, which allows to compare the results of the calculation with the real displacement. The capture was done with different materials: brushed metal, unevenly rusted metal, light wood, printer paper, black electrical tape, and microfiber cloth.

Each image was analyzed to find the laser spot center. A preliminary step is to attenuate sensor noise. First, the black threshold, $0 \leqslant t \leqslant 1$, is estimated for each image using the average intensity, excluding a strip containing the laser spot, whose position is estimated using the centroid. Each pixel value $0 \leqslant m_{ij} \leqslant 1$ is corrected for the black threshold by

$$n_{ij} = \max\left(0, m_{ij} - t\right) . \tag{2}$$

For the experiments with the slit, and without loss of generality, the strip was chosen to be 128 pixels wide, and 600 pixels high—the complete height of the captured image. Because the pattern is circular with the lens, a wider 320×600 region was retained.

Ross describes some typical ways of finding the center of a laser spot captured with a lens [32]. We chose the least squares regression of the Gaussian function

$$\mathrm{e}^{-||r||^2} , \tag{3}$$

where r is a linear transformation applied to the coordinates of the image plane:

$$r = \begin{bmatrix} \sigma_{xx} & \sigma_{xy} \\ \sigma_{yx} & \sigma_{yy} \end{bmatrix} \begin{bmatrix} x - \mu_x \\ y - \mu_y \end{bmatrix} . \tag{4}$$

We explicitly fit for the covariances σ_{xx}, σ_{xy}, σ_{yx}, σ_{yy}, and the center of the spot in the image (μ_x, μ_y).

For images captured with the slit, we compute the horizontal center for each line using the least squares regression of the Gaussian function

$$\mathrm{e}^{-\left(\frac{x-\mu}{\sigma}\right)^2} , \tag{5}$$

and finally average all the centers. Averaging the centers should cancel part of the errors from the true center, thus providing a better approximation. The algorithm only needs to determine the horizontal center, since, by hypothesis, the diffraction pattern moves only horizontally.

Table I. Error Measurement Values

Material	Lens MAX µm	Lens MAE µm	Slit MAX µm	Slit MAE µm
Brushed Metal	904	182	509	114
Rusty Metal	777	167	651	158
Light Wood Plank	651	151	429	71
Printer Paper	716	144	466	81
Black Electric Tape	1197	274	732	136
Microfiber Fabric	646	156	592	122

IV. Results

After fitting Eq. (1) using a least squares regression on the lens and slit centers, we compute the error between the model predictions and the actual target distances. Fig. 4 shows an example of these differences. In Fig. 4a, the spike near the middle of the graph is mostly explained by lens flare, while the lens distortion influences the fit in the range's extremities. In contrast, Fig. 4b show that the slit is much less affected by internal reflection and free of lens distortion. Fig. 4b, however, show some degradation

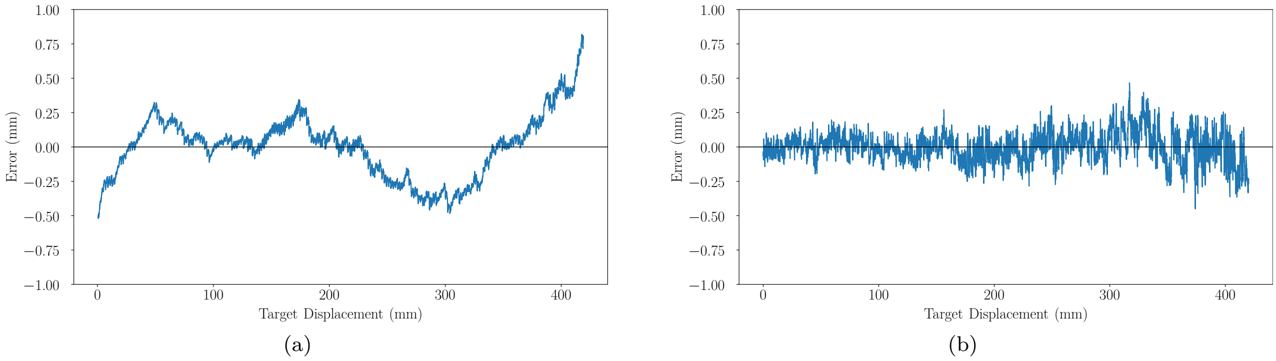

Figure 4. Model prediction errors for (a) lens captures and (b) slit captures on white paper.

in prediction quality as the target moves away. This may be partly due to the fact that the capture with a slit is darker than with a lens. As the target moves away, it becomes more difficult to detect, especially if the target is poorly reflective. Table I compares and summarizes the prediction errors of the lens and the slit according to the maximum deviation (MAX) and mean absolute error (MAE) measures with different materials.

V. Conclusion

It can be seen that the lens capture is sensitive to optical aberrations of distortion and lens flare, while the slit is not. This is especially relevant on the border of the camera sensor, and combined with a naturally wider viewing angle, the slit offers a better capture range. Although it is slightly less precise than the lens, it is overall more accurate. The error metrics show that the slit is still better in average, confirming our hypothesis.

However, precision and accuracy are limited by the nature of the surfaces. For example, rusty metal and microfiber cloth yield less accurate readings than other materials, but the slit is still better than the lens, as we can see in Table I. This is expected since highly textured and heterogeneous surfaces are problematic for laser triangulation in general [8]. This issue is exacerbated for the slit, as these surfaces also amplify laser speckle.

The slit simplifies triangulation sensors, both in hardware and in software. One could imagine a sensor made only of a laser, a filter for the wavelength of this laser, a vertical slit and a photosensitive sensor. Manufacturing would be simpler and less expensive, and very likely for better accuracy.

Some disadvantages of using a slit instead of a lens is that the image is darkened and affected by speckle noise, which lowers the signal-to-noise ratio. When using a material that absorbs a lot of light and is far from the sensor, it can be harder to precisely detect the laser spot, reducing the sensor range. It would be interesting to further study and better quantify the signal-to-noise ratio of the lens and the slit and compare the results. This problem could be mitigated by using a more sensitive light sensor, by using a brighter laser, or by using a longer exposure time, for example. Furthermore, a shorter wavelength laser (e.g. ultraviolet) could reduce the speckle and provide a better resolution as well.

A possible software improvement could be to model the laser spot more accurately, for example using the Fraunhofer, or the Fresnel approximations [33], which would take into account the diffraction pattern fringes and might help with the sensor precision. It would also be interesting to explore different laser shapes, such as Micro-Epsilon's optoNCDT LL speckle-less line sensor. It might also be intriguing to see if the slit is viable in a material profiling context with a laser profile sensor, rather than a laser point sensor.

VI. Acknowledgments

We would like to thank Suzie Loubert, mechanical engineer at UQAR, for her drawings of the experimentation table. We would also like to thank Richard Lafrance, mechanical technician at UQAR, for the assembly of the table, and Jean-Charles Morin, electrical technician at UQAR, for his help in repairing the circuit of the table's motor.

References

[1] F. Blais, "Review of 20 years of range sensor development," Journal of Electronic Imaging, vol. 13, no. 1, p. 231, Jan. 2004.

[2] M. Antonio, "Three dimensional camera and range finder," U.S. Patent 5 081 530A, Jan., 1992.

[3] S. Hsu, S. Acharya, A. Rafii, and R. New, "Performance of a time-of-flight range camera for intelligent vehicle safety applications," in Advanced Microsystems for Automotive Applications 2006, J. Valldorf and W. Gessner, Eds. Berlin, Heidelberg: Springer, 2006, pp. 205–219.

[4] S. Gokturk, H. Yalcin, and C. Bamji, "A time-of-flight depth sensor—system description, issues and solutions," in 2004 Conference on Computer Vision and Pattern Recognition Workshop. IEEE, 2004, p. 35.

[5] T. Bosch, “Laser ranging: a critical review of usual techniques for distance measurement,” Optical Engineering, vol. 40, no. 1, pp. 10–19, Jan. 2001.

[6] S. V. F. Barreto, R. E. Sant’Anna, and M. A. F. Feitosa, “A method for image processing and distance measuring based on laser distance triangulation,” in IEEE 20th International Conference on Electronics, Circuits, and Systems (ICECS), 2013, pp. 695–698.

[7] T. A. Clarke, K. T. V. Grattan, and N. E. Lindsey, “Laser-based triangulation techniques in optical inspection of industrial structures,” in Optical Testing and Metrology III: Recent Advances in Industrial Optical Inspection, C. P. Grover, Ed., vol. 1332. SPIE, Jan. 1991, pp. 474–486.

[8] A. Donges and R. Noll, Laser Measurement Technology. Springer Berlin Heidelberg, 2015.

[9] Z. Ji and M. Leu, “Design of optical triangulation devices,” Optics & Laser Technology, vol. 21, no. 5, pp. 339–341, 1989.

[10] S. Kumar, P. K. Tiwari, and S. Chaudhury, “An optical triangulation method for non-contact profile measurement,” in 2006 IEEE International Conference on Industrial Technology. IEEE, 2006, pp. 2878–2883.

[11] N. Swojak, M. Wieczorowski, and M. Jakubowicz, “Assessment of selected metrological properties of laser triangulation sensors,” Measurement, vol. 176, May 2021.

[12] T. Scheimpflug, “Improved Method and Apparatus for the Systematic Alteration or Distortion of Plane Pictures and Images by Means of Lenses and Mirrors for Photography and for other purposes,” G.B. Patent 190 401 196A, May, 1904.

[13] S.-J. Lee and D.-Y. Chang, “A laser sensor with multiple detectors for freeform surface digitization,” The International Journal of Advanced Manufacturing Technology, vol. 31, no. 11–12, pp. 1181–1190, Jul. 2006.

[14] F.-J. Shiou and M.-X. Liu, “Development of a novel scattered triangulation laser probe with six linear charge-coupled devices (CCDs),” Optics and Lasers in Engineering, vol. 47, no. 1, pp. 7–18, Jan. 2009.

[15] Y. Selami, W. Tao, Q. Gao, H. Yang, and H. Zhao, “A scheme for enhancing precision in 3-dimensional positioning for non-contact measurement systems based on laser triangulation,” Sensors, vol. 18, no. 2, art. 504, Feb. 2018.

[16] G. Bickel, G. Häusler, and M. Maul, “Triangulation with expanded range of depth,” Optical Engineering, vol. 24, no. 6, pp. 975–977, Dec. 1985.

[17] G. Häusler and W. Heckel, “Light sectioning with large depth and high resolution,” Applied Optics, vol. 27, no. 24, pp. 5165–5169, Dec. 1988.

[18] K. Žbontar, M. Mihelj, B. Podobnik, F. Povše, and M. Munih, “Dynamic symmetrical pattern projection based laser triangulation sensor for precise surface position measurement of various material types,” Applied Optics, vol. 52, no. 12, pp. 2750–2760, Apr. 2013.

[19] P. Kienle, L. Batarilo, M. Akgül, M. H. Köhler, K. Wang, M. Jakobi, and A. W. Koch, “Optical Setup for Error Compensation in a Laser Triangulation System,” Sensors, vol. 20, no. 17, art. 4949, Sep. 2020.

[20] G. Ye, Y. Zhang, W. Jiang, S. Liu, L. Qiu, X. Fan, H. Xing, P. Wei, B. Lu, and H. Liu, “Improving measurement accuracy of laser triangulation sensor via integrating a diffraction grating,” Optics and Lasers in Engineering, vol. 143, art. 106631, Apr. 2021.

[21] R. G. G.-A. na and H. A. Chaparro-Romo, “General formula for bi-aspheric singlet lens design free of spherical aberration,” Applied Optics, vol. 57, no. 31, pp. 9341–9345, Nov. 2018.

[22] M. Young, “Pinhole optics,” Applied Optics, vol. 10, no. 12, pp. 2763–2767, Dec. 1971.

[23] M. Young, “Pinhole imagery,” American Journal of Physics, vol. 40, no. 5, pp. 715–720, May 1972.

[24] J. M. Franke, “Field-widened pinhole camera,” Applied Optics, vol. 18, no. 17, p. 2913, Sep. 1979.

[25] T. Hsu, “Reflective wide-angle pinhole camera,” Applied Optics, vol. 21, no. 13, p. 2303, Jul. 1982.

[26] S. G. B. Airy, On the Diffraction of an Object-glass with Circular Aperture. Printed at the Pitt Press by John Smith, Jan. 1835, vol. V, no. III.

[27] R. Baribeau and M. Rioux, “Influence of speckle on laser range finders,” Applied Optics, vol. 30, no. 20, pp. 2873–2878, Jul. 1991.

[28] R. Baribeau and M. Rioux, “Centroid fluctuations of speckled targets,” Applied Optics, vol. 30, no. 26, pp. 3752–3755, Sep. 1991.

[29] R. G. Dorsch, G. Häusler, and J. M. Herrmann, “Laser triangulation: fundamental uncertainty in distance measurement,” Applied Optics, vol. 33, no. 7, pp. 1306–1314, Mar. 1994.

[30] 1.3 MP Custom Lens CMOS Global Shutter Camera Module (Monochrome), e-con Systems, Apr. 2013. [Online]. Available: https://www.e-consystems.com/1MP-USB3-Globalshutter-Camera.asp

[31] 1/3-inch 1.2 Mp CMOS Digital Image Sensor with Global Shutter, onsemi, May 2022, rev. 11. [Online]. Available: https://www.onsemi.com/pdf/datasheet/ar0134cs-d.pdf

[32] T. S. Ross, Laser Beam Quality Metrics. Bellingham, Washington 1000 20th St. Bellingham WA 98225-6705 USA: SPIE, 2013.

[33] M. Born, E. Wolf, A. B. Bhatia, P. C. Clemmow, D. Gabor, A. R. Stokes, A. M. Taylor, P. A. Wayman, and W. L. Wilcock, Principles of Optics. Cambridge University Press, Oct. 1999.